**EPJ manuscript No.**
(will be inserted by the editor)

# Universal behavior of baryons and mesons transverse momentum distributions in the framework of percolation of strings

L. Cunqueiro[1], J.Dias de Deus[2], E. G. Ferreiro[1], and C. Pajares[1]

[1]Instituto Galego de Física de Altas Enerxías and Departamento de Física de Partículas, Universidade de Santiago de Compostela, 15782 Santiago de Compostela, Spain.
[2] CENTRA, Instituto Superior Técnico, 1049-001 Lisboa, Portugal

Agosto. 1, 2007

**Abstract.** In the framework of percolation of strings, the transverse momentum distributions in AA and hh collisions at all centralities and energies follow a universal behavior. The width of these distributions is related to the width of the distribution of the size of the clusters formed from the overlapping of the produced strings. The difference between the distributions for baryons and mesons originates in the fragmentation of clusters of several strings which enhance the particles with higher number of constituents. The results agree with SPS and RHIC data. The predictions for LHC show differences for baryons compared with RHIC. At LHC energies we obtain also a high pt suppression for pp high multiplicity events compared with pp minimum bias.

**PACS.** 25.75.Nq – 12.38.Mh – 24.85+p



Multiparticle production can be described in terms of color strings stretched between the partons of the projectile and target. These strings decay into new ones by sea $q-\overline{q}$ pair production and subsequently hadronize to produce the observed hadrons. The color in these strings is confined to a small area in transverse space: $S_1 = \pi r_0^2$ with $r_0 \simeq 0.2 - 0.3$ fm. With increasing energy and/or atomic number of the colliding particles, the number of exchanged strings grows and they start to overlap , forming clusters, very much like disks in two-dimensional percolation theory. At a certain critical density, a macroscopical cluster appears, which marks the percolation phase transition [1, 2]. For nuclear collisions, this density corresponds to the value of $\eta = N_S \frac{S_1}{S_A}$ of $\eta_C = 1.18 - 1.5$(depending of the type of the employed profile functions) where $N_S$ is the number of strings and $S_A$ corresponds to the overlapping area of the nuclei. A cluster of n strings behaves as a single string with and energy-momentum that corresponds to the sum of the energy-momentum of the overlapping strings and with a higher color field, corresponding to the vectorial sum of the color fields of the individual strings. In this way, the multiplicity $< \mu_n >$ and the mean transverse momentum squared $< p_T^2 >_n$ of the particles produced by a cluster are given by

$$< \mu >_n = \sqrt{\frac{nS_n}{S_1}} < \mu >_1 \qquad < p_T^2 >_n = \sqrt{\frac{nS_1}{S_n}} < p_T^2 >_1 \tag{1}$$

where $< \mu >_1$ and $< p_T^2 >_1$ stand for the mean multiplicity and mean $p_T^2$ of particles produced in a single string. Eqs.1 transform into analytical ones [2] in the limit of random distributions of strings

$$< \mu >= N_S F(\eta) < \mu >_1 \qquad < p_T^2 >= \frac{< p_T^2 >_1}{F(\eta)} \tag{2}$$

where $F(\eta) = \sqrt{\frac{1-e^{-\eta}}{\eta}}$. If we are interested in a determined kind of particle i, we will use $< \mu >_{1i}$, $< p_T^2 >_{1i}$ $< \mu >_{ni}$ and $< p_T^2 >_{ni}$ for the corresponding quantities. The transverse momentum distributions can be written as a superposition of the transverse momentum distributions of each cluster, $g(x, p_T)$, weighted with the distribution of the different tension of the clusters, i.e the distribution of the size of the clusters, $W(x)$ [3,4]. For $g(x, p_T)$ we assume the Schwinger formula $g(x, p_T) = exp(-p_T^2 x)$ and for the weight function $W(x)$, the gamma distribution $W(x) = \frac{\gamma}{\Gamma(k)}(\gamma x)^{k-1} exp(-\gamma x)$ where

$$\gamma = \frac{k}{< x >} \qquad \frac{1}{k} = \frac{< x^2 > - < x >^2}{< x >^2}.$$

$x$ is proportional to the inverse of the tension of each cluster, precisely $x = 1/ < p_T^2 >_n = \sqrt{\frac{S_n}{nS_1}} \frac{1}{<p_T^2>}$. $k$ is proportional to the inverse of the width of the distribution on $x$ and depends on $\eta$, the density of strings. Therefore, the transverse momentum distribution $f(p_T, y)$ is

$$\frac{dN}{dp_T^2 dy} = f(p_T, y) = \int_0^\infty dx W(x) g(p_T, x) =$$

$$\frac{dN}{dy}\frac{k-1}{k}\frac{1}{<p_T^2>_{1i}}F(\eta)\frac{1}{(1+\frac{F(\eta)p_T^2}{k<p_T^2>_{1i}})^k} \quad (3)$$

Eq.(3) is valid for all densities and type of collisions. It only depends on the parameters $<p_T>_{1i}$ and k. At low density, there is no overlapping between strings and there are no fluctuations on the string tension , all the clusters have one string. Therefore, k goes to infinity, and $f(p_T,y) \simeq exp(-\frac{p_T^2}{<p_T^2>_1})$. At very high density $\eta$, there is only one cluster formed by all the produced strings. Again, there are no fluctuations, k tends to infinity and $f(p_T,y) \simeq exp(-\frac{F(\eta)p_T^2}{<p_T^2>_1})$ . In between these two limits, k has a minimum for intermediate densities corresponding to the maximum of the cluster size fluctuations. This behavior of k with $\eta$ [3,4] is related to the behavior with centrality of the transverse momentum [5] and multiplicity fluctuations [6]. We observe from eq.(3) that

$$\frac{dlnf(p_T^2,y)}{dlnp_T} = -\frac{2F(\eta)}{(1+\frac{2F(\eta)p_T^2}{k<p_T^2>_i})}\frac{p_T^2}{<p_T^2>_{1i}} \quad (4)$$

As $p_T^2 \longrightarrow 0$, eq.(4) reduces to $\frac{-2F(\eta)p_T^2}{<p_T^2>_i}$ while for larger $p_T$ it becomes $-2k$ for all particle species. As $<p_T^2>_{1p} \geq <p_T^2>_{1K} \geq <p_T^2>_{1\pi}$, the absolute value is larger for pions than for kaons and for protons, in agreement with experimental data [3].

The nuclear modification factor , defined as $R_{AA}(p_T) = \frac{dN^{AA}}{dp_T^2 dy}/N_{coll}\frac{dN^{pp}}{dp_T^2 dy}$, reduces to the following expression at $p_T^2 = 0$ (we use eq.2 for $\frac{dN}{dy}$):

$$R_{AA}(0) \sim (\frac{F(\eta')}{F(\eta)})^2 < 1 \quad (5)$$

where $\eta'$ and $\eta$ are the corresponding densities for nucleus-nucleus collisions and pp collisions respectively. $\eta' > \eta$, thus $F(\eta') < F(\eta)$. As $p_T$ increases we have

$$R_{AA}(p_T) \sim \frac{1+F(\eta)\frac{p_T^2}{<p_T^2>_{1i}}}{1+F(\eta')\frac{p_T^2}{<p_T^2>_{1i}}}(\frac{F(\eta')}{F(\eta)})^2 \quad (6)$$

and $R_{AA}$ increases with $p_T$ up to a maximum value. At larger $p_T$ ($\frac{p_T^2}{k<p_T^2>_{1i}}F(\eta) > 1$)

$$R_{AA} \sim p_T^{2(k(\eta)-k'(\eta'))} \quad (7)$$

At high density $k'(\eta') > k(\eta)$ and suppression of $p_T$ occurs.

The universal formula (3) must be regarded as an analytical approximation to a process which consists on the formation of clusters of strings and their eventual decay via the Schwinger mechanism. We do not claim to have an alternative description valid at all $p_T$. It is well known that jet quenching is the working mechanism responsible of the high $p_T$ suppression. This phenomena is not included in our formula which was obtained assuming a single exponential for the decay of a cluster without a power like tail. Our work must be considered as an interpolating way of joining smoothly the low and intermediate $p_T$ region with the high $p_T$ region. The suppression of high $p_T$ has correspondence with a modification in the behavior at intermediate $p_T$ and this is what we study. Although it describes many of the observed features of experimental SPS and RHIC data, it is not able to explain the differences between antibaryons(baryons) and mesons. In fact, the only different parameter between them in formula(3) is the mean transverse momentum of pions and protons produced by a single string $<p_T^2>_{1\pi}$ and $<p_T^2>_{1p}$ respectively. This only causes a shift on the maximum of $R_{AA}$ but keeps the same height at the maximum contrary to the observed. However, in the fragmentation of a cluster formed by several strings, the enhancement of the

production of antibaryons(baryons) over mesons is not only due to a mass effect corresponding to a higher tension due to higher density of the cluster(factor $F(\eta)$in front of $p_T^2$ in formula(3)). In fact, the color and flavor properties of a cluster follow from the corresponding properties of their individual strings. A cluster composed of several quark-antiquarks $(q-\overline{q})$ strings behaves like a $(Q-\overline{Q})$ string, with a color Q and flavor composed of the flavor of the individual strings. As a result, we obtain clusters with higher color and differently flavored ends. For the fragmentation of a cluster we consider the creation of a pair of parton complexes $Q\overline{Q}$ [7]. After the decay, the two new $Q\overline{Q}$ strings are treated in the same manner and therefore decay into more $Q\overline{Q}$ strings until they come to objects with masses comparable to hadron masses which are identified with observable hadrons by combining into them the produced flavor with statistical weights. In this way, the production of antibaryons(baryons) is enhanced with the number of strings of the cluster. As an example, in fig.1 we show the results for the decay of a color octet cluster and color sextet formed by two $3-\overline{3}$ strings [7], were there is a large enhancement of antibaryons(baryons). Notice that the enhancement of strangeness with zero baryon number is smaller [7,8,9]. We observe that the additional antiquarks (quarks) required to form an (anti)baryon are provided by the antiquarks(quarks) of the overlapping strings which form the cluster. In this way, the recombination and coalescence ideas [10] are naturally incorporated in our approach. In order to take this into account in our formulas, we must modify the eqs.(1),(2) and (3). For (anti)baryons we will consider the multiplicity per unit of rapidity to be instead of the first equation of 2:

$$\mu_{\overline{B}} = N_S^{1+\alpha}F(\eta_{\overline{B}})\mu_{1\overline{B}} \quad (8)$$

fitting the parameter $\alpha$ to reproduce the experimental dependence of the pt integrated $\overline{p}$ spectra with centrality [11]. The result is shown in fig.2 and the obtained values are $\alpha = 0.09$ and $\frac{\mu_{1\overline{p}}}{\mu_{1\overline{\pi}}} = \frac{1}{30}$. $\mu_{1\overline{p}}$ and $\mu_{1\overline{\pi}}$ are the mean multiplicity of a single string for anitprotons and pions respectively. It is observed that when an antibaryon is triggered, the effective number of strings is $N_S^{1+\alpha}$ instead of $N_S$. This means that the density $\eta$ must be replaced by $\eta_{\overline{B}} = N_S^{\alpha}\eta$. The (anti)baryons probe a higher density than mesons for the same energy and type of collision. On

the other hand, from constituent counting rules [12] it is expected that the power-like $p_T$ behavior for baryons is suppressed in one half more than mesons. Therefore, in (3) we must use for (anti)baryons $\eta_B$ and the corresponding functions $F(\eta_B)$ and $k_B = k(\eta_B) + \frac{1}{2}$. Since $\eta_B > \eta$ we have $F(\eta_B) < F(\eta)$ and $k(\eta_B) > k(\eta)$. For peripheral collisions, $N_S^\alpha$ is smaller than for central collisions and $\eta_B$ is more similar to $\eta$. Therefore, the differences between the transverse momentum distributions are smaller as it is shown by the experimental data. In order to compute the different $\eta$s for different centralities we use the Monte-Carlo code of references [7,8]. Their values at RHIC and LHC and their corresponding k's are tabulated below. Note that the values of k come from the universal function which gives the shape of the dependence of k on $\eta$ [3,4].

In our approach, we should use a different $\alpha$ for baryons and antibaryons as far as the increase with centrality is slightly different for both, depending also on the specific kind of baryon(antibaryon). In order to obtain a single formula we considered strings of the same type. However, usually two types of strings are considered. Strings $qq-q$ or $q-qq$ which stretch a diquark of the projectile (target) with a quark of the target(projectile) and strings $q-\overline{q}$ or $\overline{q}-q$ linking quarks and antiquarks. The fragmentation of the strings of the type $qq-q$ or $q-qq$ favors the production of baryons over antibaryons in the fragmentation regions of the projectile and the target. Therefore our results should be limited to the central rapidity region. On the other hand, we have determined $\alpha$ from the dependence of $\frac{\overline{p}}{\pi}$ with centrality. The large error data translate into uncertanties in $\alpha$ of the order of 20% which is of the same order of the differences in the parameter $\alpha$ for baryons and antibaryons. The uncertanties in $\alpha$ induce uncertanties in the determination of $\eta_B$ and hence in $k_B$; these uncertanties are however negligible (less than 5% even at the highest centrality). We conclude that our single formula using the same $\alpha$ for baryons and antibaryons is a good approximation.

On the other hand, we have assumed an additional difference between baryons and mesons, $k_B = k(\eta_B) + 1/2$, from the high $p_T$ behavior of eq.3. This could seem inconsistent with our approach that is limited to low and intermediate $p_T$. As we have said above, our goal is not to give a full description of data, including high $p_T$ but an alternative description of intermediate $p_T$ suppression. In this way, this factor can be seen as a boundary condition imposed to our approach. Notice that this factor is independent of the centrality and therefore its influence on the ratios $R_{CP}$ and $R_{AA}$ is not large. In fact, if we use for $k_B$ the values without the factor 1/2, $R_{CP}$ is smaller at $p_T = 2$ GeV/c and $p_T = 10$ GeV/c in a factor 1.13 and 1.25 respectively at RHIC energies. This small reduction does not spoil the agreement with data although a better agreement at high $p_T$ is obtained with the 1/2 factor.

In fig 3., we show our results for the ratio $R_{CP}$ in Au-Au collisions defined as usual, for $(p+\overline{p})/2$ (dashed line) and neutral pions(solid line), compared to the PHENIX [11] experimental data. We find a good agreement. We also show the LHC prediction for pions and antiprotons. There is no change for pions but on the contrary, the difference between antibaryons and pions is enhanced. In fig.4 we show the $p_T$ dependence of the ratio $\frac{\overline{p}}{\pi^0}$ for peripheral (dashed line) and central (solid line) Au-Au collisions together with experimental data [11]. LHC predictions are also shown. The difference only appears for central collisions.

In fig.5 we show our results for the modified nuclear factor $R_{AA}$ for pions (solid lines) and protons (dashed lines) for peripheral and central collisions together with the experimental data for pions([13]). Again, the main difference arises for central collisions. In fig.6, this difference between pions and protons is compared at RHIC and LHC energies. The Cronin effect becomes larger at LHC for protons, contrary to some expectations[14].

The good agreement obtained with the experimental data can be understood as two combined effects:the larger string tension of the cluster and the formation of strong color fields[15] and the way of fragmentation of the clusters which enhances (anti)baryon over mesons similarly to recombination models[10]. Both effects are widely recognized as working physical mechanisms at high densities . Both effects are naturally incorporated in the percolation of strings approach.

The shape of $R_{AA}$ and $R_{CP}$ has nothing to do with the nucleon structure of the nucleus an it depends essentially on the string density. One can wonder whether in pp at LHC energies can be reached enough string densities to get a high $p_T$ suppression. In fig. 7 we answer this question. It is plotted the ratio $R_{CP}$ between the inclusive pp going to $\pi$, $k$ and $\overline{p}$ cross section for events with a multiplicity twice higher than the mean multiplicity and the minimum bias cross section. It is observed a suppression for $p_T$ larger than 3 GeV/c. However, the reached string density in pp collisions will not be enough to suppress the back to back jet correlations as observed at RHIC energies for Au-Au central collisions. A straightforward evaluation following [3], gives a maximum of absorption of $\Delta p_T = 2$ GeV/c for a number of strings of the order of 25-30 corresponding to events with a multiplicity twice the minimum bias multiplicity.

We thank Ministerio de Educación y Ciencia of Spain under project FPA2005-01963 and Conselleria de Educación da Xunta de Galicia for financial support. We thank N.Armesto, C.Salgado and Y.Shabelski for discussions.

## References

1. N. Armesto, M. A. Braun, E. G. Ferreiro and C. Pajares, Phys. Rev. Lett. **77** (1996) 3736; M. Nardi and H. Satz, Phys. Lett. B **442** (1998) 14.
2. M. A. Braun and C. Pajares, Phys. Rev. Lett. **85** (2000) 4864; Eur.Phys.J C**85**,349 (2000).
3. J. Dias de Deus, E. G. Ferreiro, C. Pajares and R. Ugoccioni, Eur. Phys. J. C **40** (2005) 229.
4. C. Pajares, Eur. Phys. J. C **43** (2005) 9; J. Dias de Deus and R. Ugoccioni, Eur. Phys. J. C **43** (2005) 249.
5. K. Adcox *et al.* [PHENIX Collaboration], Nucl. Phys. A **757** (2005) 184; E. G. Ferreiro, F. del Moral and C. Pa-

| Centrality | $\eta$ | $k$ | $\eta_B$ | $k_B$ |
|---|---|---|---|---|
| RHIC | | | | |
| Au-Au $0-10\%$ | 2.69 | 3.97 | 5.17 | 4.82 |
| Au-Au $60-92\%$ | 0.9 | 3.58 | 1.24 | 4.16 |
| Au-Au $80-92\%$ | 0.6 | 3.55 | 0.75 | 4.06 |
| pp | 0.4 | 3.60 | 0.48 | 4.07 |
| LHC | | | | |
| Au-Au $0-10\%$ | 4.85 | 4.07 | 9.8 | 4.99 |
| Au-Au $60-92\%$ | 1.62 | 3.56 | 2.34 | 4.21 |
| Au-Au $80-92\%$ | 1.08 | 3.44 | 1.43 | 4.02 |
| pp | 0.72 | 3.38 | 0.92 | 3.90 |

**Table 1.** Density of strings and the corresponding k values for mesons and barions at RHIC and LHC.

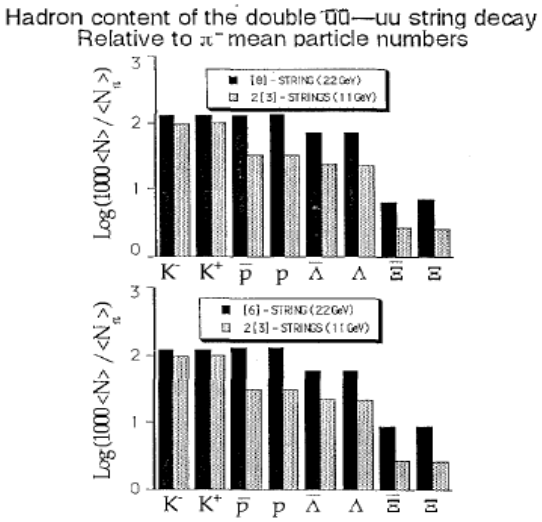


**Fig. 1.** Hadronic content of the decay of octet and sextet strings relative to the number of $\pi^-$.

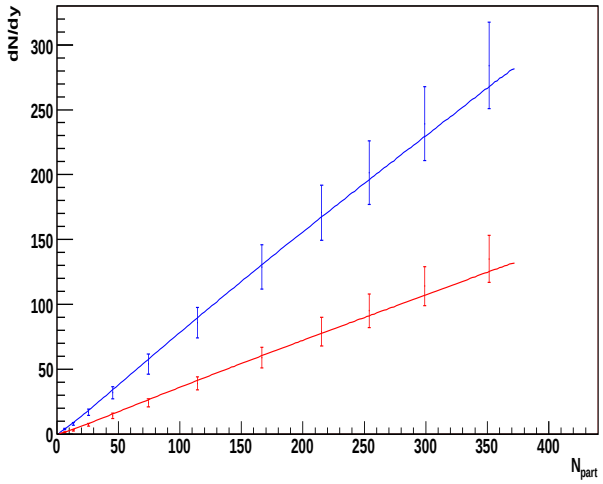


**Fig. 2.** $p_T$ integrated antiproton(red, X 10) and neutral pion (blue) spectra as a function of centrality compared to PHENIX data.

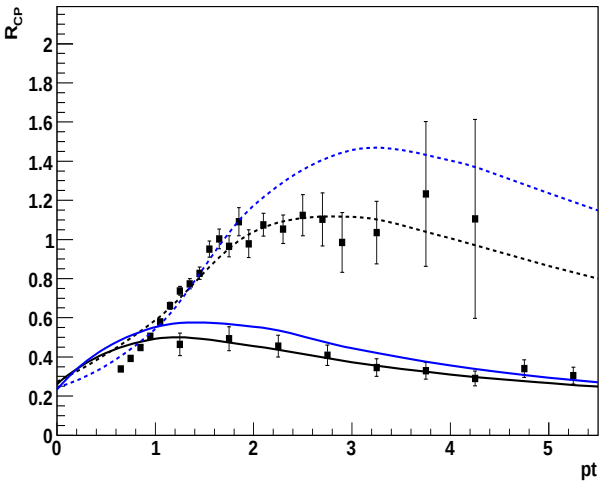


**Fig. 3.** $R_{CP}$(0-10% central/60-92% peripheral) for pions (solid line) and $(p+\overline{p})/2$ (dashed) compared to PHENIX data. In blue, LHC predictions.

jares, Phys. Rev. C **69** (2004) 034901; J. Dias de Deus and A. Rodrigues, arXiv:hep-ph/0308011.

6. C. Alt *et al.* [NA49 Collaboration], Phys. Rev. C **75** (2007) 064904; L. Cunqueiro, E. G. Ferreiro, F. del Moral and C. Pajares, Phys. Rev. C **72** (2005) 024907.
7. N. S. Amelin, M. A. Braun and C. Pajares, Z. Phys. C **63** (1994) 507.
8. N. Armesto, C. Pajares and D. Sousa, Phys. Lett. B **527** (2002) 92.
9. H. J. Mohring, J. Ranft, C. Merino and C. Pajares, Phys. Rev. D **47** (1993) 4142; C.Greiner AIP Conf. Proc.644,337 (2003) nucl-th/0208080.
10. R. C. Hwa and C. B. Yang, Phys. Rev. C **69** (2004) 034902; V. Greco, C. M. Ko and P. Levai, Phys. Rev. Lett. **90** (2003) 202302; R. J. Fries, B. Muller, C. Nonaka and S. A. Bass, Phys. Rev. Lett. **90** (2003) 202303; R. J. Fries, B. Muller, C. Nonaka and S. A. Bass, Phys. Rev. C **68** (2003) 044902; L. Maiani, A. D. Polosa, V. Riquer and C. A. Salgado, Phys. Lett. B **645** (2007) 138.
11. S. S. Adler *et al.* [PHENIX Collaboration], Phys. Rev. C **69** (2004) 034909.
12. S. J. Brodsky and G. R. Farrar, Phys. Rev. Lett. **31** (1973) 1153; V.A.Matreev,R.M.Murddyan, A.N.Tavkheldize Lett. Nuuovo Cimento **7**, 719(1973); G. P. Lepage and S. J. Brodsky, Phys. Rev. D **22** (1980) 2157.
13. S. S. Adler *et al.* [PHENIX Collaboration], Phys. Rev. Lett. **91** (2003) 072301.
14. J. L. Albacete, N. Armesto, A. Kovner, C. A. Salgado and U. A. Wiedemann, Phys. Rev. Lett. **92** (2004) 082001.
15. V. Topor Pop, M. Gyulassy, J. Barrette, C. Gale, S. Jeon and R. Bellwied, Phys. Rev. C **75** (2007) 014904; E. L. Bratkovskaya *et al.*, Phys. Rev. C **69** (2004) 054907;

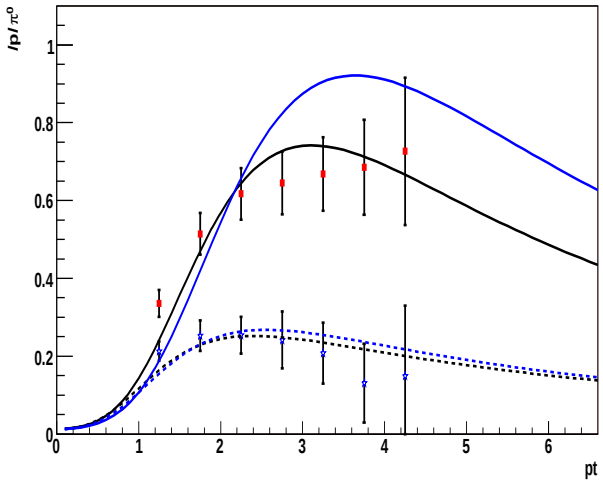


**Fig. 4.** Antiproton to neutral pion ratio as a function of $p_T$ for for 0-10% (solid) and 60-92% (dashed) centrality bins compared to PHENIX data. LHC predictions in blue.

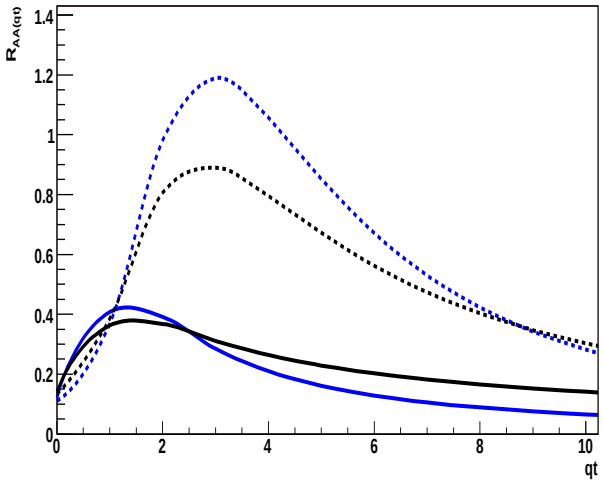


**Fig. 6.** Nuclear modification factor for 0-10% central pions (solid) and protons (dashed) at RHIC (black) and LHC (blue)

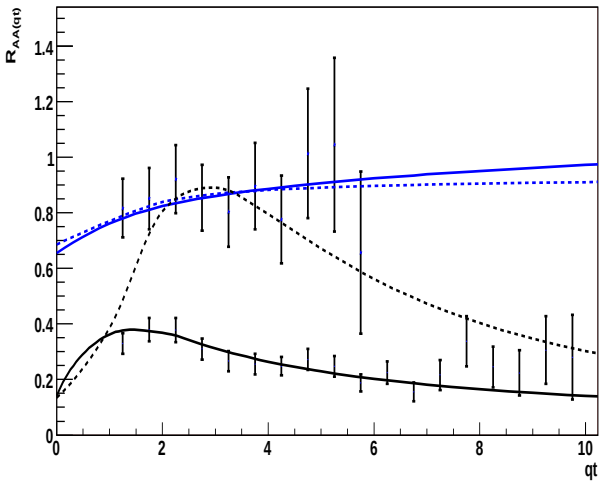


**Fig. 5.** Nuclear modification factor for neutral pions (solid) and protons (dashed) for 0-10% central and 80-92% peripheral bins compared to PHENIX data.

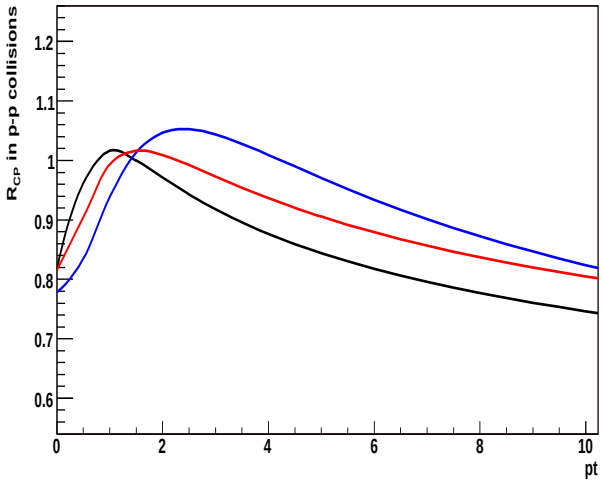


**Fig. 7.** Central to peripheral ratio for pp collisions at LHC. Black: $\pi^0$, Red: kaons, Blue: $\overline{p}$